THE JOURNAL OF PHYSICAL CHEMISTRY Letters

Letter

pubs.acs.org/JPCL

Dissociative Water Adsorption by $Al_3O_4^+$ in the Gas Phase

Matias R. Fagiani,[†,‡] Xiaowei Song,[†,‡] Sreekanta Debnath,[†,‡] Sandy Gewinner,[‡] Wieland Schöllkopf,[‡] Knut R. Asmis,*[,†] Florian A. Bischoff,[§] Fabian Müller,[§] and Joachim Sauer*[,§]

[†]Wilhelm-Ostwald-Institut für Physikalische und Theoretische Chemie, Universität Leipzig, Linnéstrasse 2, D-04103 Leipzig, Germany

[‡]Fritz-Haber-Institut der Max-Planck-Gesellschaft, Faradayweg 4-6, D-14195 Berlin, Germany

[§]Institut für Chemie, Humboldt-Universität zu Berlin, Unter den Linden 6, D-10099 Berlin, Germany

Supporting Information

ABSTRACT: We use cryogenic ion trap vibrational spectroscopy in combination with density functional theory (DFT) to study the adsorption of up to four water molecules on $Al_3O_4^+$. The infrared photodissociation spectra of $[Al_3O_4(D_2O)_{1-4}]^+$ are measured in the O−D stretching (3000−2000 cm^{-1}) as well as the fingerprint spectral region (1300−400 cm^{-1}) and are assigned based on a comparison with simulated harmonic infrared spectra for global minimum-energy structures obtained with DFT. We find that dissociative water adsorption is favored in all cases. The unambiguous assignment of the vibrational spectra of these gas phase model systems allows identifying characteristic spectral regions for O−D and O−H stretching modes of terminal (μ_1) and bridging (μ_2) hydroxyl groups in aluminum oxide/water systems, which sheds new light on controversial assignments for solid Al_2O_3 phases.

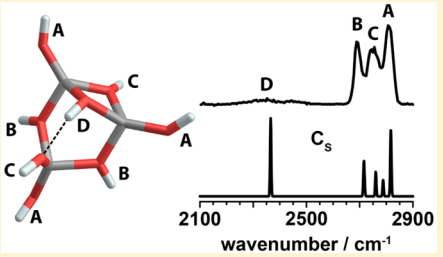

Alumina-based materials are used in many technological and environmental applications, e.g., as catalysts and catalyst supports, coatings, abrasives, and nanosensors.[1−3] In these applications the interaction of the alumina surfaces with water is crucial,[4,5] but our molecular-level understanding of alumina−water interactions is limited, in particular because of the multiscale nature of the processes involved as well as difficulties in preparing clean surfaces with a well-defined surface termination. In spite of substantial progress with surface science techniques such as vibrationally resonant sum-frequency generation (VSF) spectroscopy,[6−8] safe assignments of the multiple bands observed in the O−H stretching region of different aluminas have not yet been achieved. For example for γ-Al_2O_3, the assignment[9] based on the classical model of Knözinger and Ratnasamy,[10] which distinguishes between terminal (μ_1) hydroxyl groups and hydroxyl groups bridging two (μ_2) or three (μ_3) Al ions has been questioned.[11]

Complementary experimental information on the vibrational signature of water adsorption can be obtained from studies on isolated aluminum oxide aggregates in the gas phase. The advantage of such model studies[12,13] on mass-selected gas-phase clusters lies in the high experimental selectivity and sensitivity, the absence of any interfering interactions with their environment, and in geometric structure information that is accessible from quantum chemical calculations.

While much spectroscopic work has been performed on bare aluminum oxide clusters in the gas phase, see e.g. ref[14−19] and references therein, previous experimental studies on their interaction with water are scarce. Jarrold and co-workers investigated the reaction of $Al_3O_3^-$ and $Al_5O_4^-$ with water by anion photoelectron spectroscopy[20−22] and found dissociative water adsorption to be energetically favored over molecular one, which was supported by computational studies.[23−26] Schwarz and co-workers studied the reactivity of the $Al_2O_7^+$ radical toward water using mass spectrometry,[27] whereas Johnson and Panas[28] used density functional theory (DFT) for calculations on reaction products of AlO(OH) and Al_2O_3 molecules with up to seven and three water molecules, respectively.

Here, we focus on the reaction of $Al_3O_4^+$ with water vapor under multiple collision conditions at room temperature. The $Al_3O_4^+$ cation was chosen because Al is fully oxidized and it has a closed-shell electronic structure,[18] thus avoiding highly reactive radicals. The vibrational spectra of $Al_3O_4^+$ with one up to four adsorbed D_2O molecules, obtained by infrared photodissociation (IRPD) spectroscopy for $n \leq 2$ (D_2-tag loss) and infrared multiple photon dissociation (IRMPD) spectroscopy for n = 3−4 (predominantly D_2O loss), are shown in Figure 1. Experimental bands are labeled with capital letters and their positions are summarized in Table S1. The spectra were measured in the O−D stretching (3000−2000 cm^{-1}) and fingerprint (1300−400 cm^{-1}) regions. As reference (broken line in Figure 1) we show the wavenumber for an isolated decoupled O−D vibration in D_2O, calculated as the average (2730 cm^{-1}) of the symmetric (υ_S, 2672 cm^{-1}) and antisymmetric (υ_{AS}, 2788 cm^{-1}) O−D stretches of a free water molecule.[29] For alumina surfaces, free terminal and bridging O−D groups resulting from dissociated water

Received: February 3, 2017
Accepted: March 1, 2017

DOI: 10.1021/acs.jpclett.7b00273
J. Phys. Chem. Lett. 2017, 8, 1272−1277

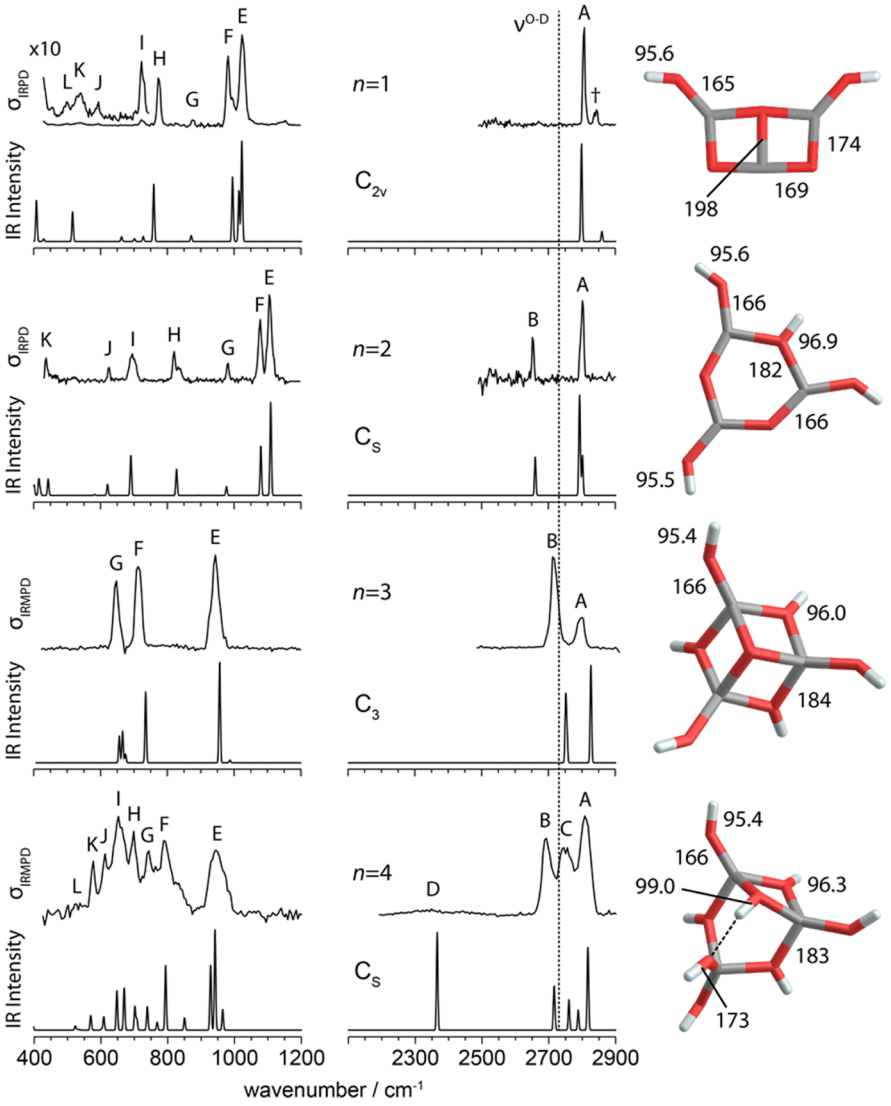

Figure 1. Vibrational spectra and global energy minimum structures of $[Al_3O_4(D_2O)_n]^+$ clusters. Selected bond distances are given in pm. For each system, the top panel shows the experimental spectrum (IRPD for n = 1, 2 and IRMPD for n = 3, 4), whereas the lower panel shows the computed (B3LYP/TZVPP) harmonic spectrum. Frequencies above 2000 cm^{-1} have been scaled with the factor 0.9732. The vertical broken line indicates the average of the experimental band positions of the antisymmetric and symmetric stretching modes of free D_2O. Experimental bands are labeled with capital letters and symbols (see text).

molecules are found between 2803 and 2715 cm^{-1},[30] while hydrogen-bonded groups are expected around 2640 cm^{-1} (estimated from the O−H stretch wavenumber of 3590 cm^{-1}).[9] In protonated water clusters, free O−D stretching modes are observed between 2800 and 2650 cm^{-1}, while hydrogen-bonded O−D stretches are red-shifted and found below 2575 cm^{-1}.[31,32]

In the fingerprint region, the observed spectra mainly contain contributions from Al−O stretching modes (ν) as well Al−O−D bending and deformation modes (δ) and allow insight into structural changes of the $Al_3O_4^+$ substrate cluster upon water adsorption. The IRPD spectrum of $Al_3O_4^+$,[18] shows absorption only below 900 cm^{-1} and its most intense feature, labeled E in Figure S4, is centered at 871 cm^{-1}. Adsorption of up to two D_2O molecules leads to a blue shift of the highest energy absorption band E in the fingerprint region from 871 cm^{-1} (n = 0), over 1023 cm^{-1} (n = 1) to 1104 cm^{-1} (n = 2). Concomitantly, a second intense band (F) appears at slightly lower energies at 971 cm^{-1} (n = 1) and 1077 cm^{-1} (n = 2). Less intense bands, labeled with G to L, are observed at lower energies. Adsorption of the third D_2O reverses the trend described for band E and leads to a simpler IR spectrum, exhibiting similarities to that of n = 0, suggesting similar structural motifs. Finally, adsorption of the fourth D_2O molecule results in a quasi-continuous absorption from about 1000 down to 500 cm^{-1} involving bands E−L.

In the O−D stretching region, adsorption of the first D_2O molecule is signaled by band A at 2806 cm^{-1}, 76 cm^{-1} higher than the reference of an isolated O−D oscillator in D_2O (2730 cm^{-1}).[29] The position of band A (see Table S1) varies only by 10 cm^{-1} between n = 1 and n = 4 (2807−2797 cm^{-1}). Upon adsorption of the second D_2O molecule a second free O−D stretching band is observed at 2651 cm^{-1} (B), 155 cm^{-1} to the red of band A. The separation between bands A and B is reduced upon addition of the third and fourth D_2O molecule. For n = 4 an intermediate band C is also observed, leading to a quasi-continuous absorption of the free O−D oscillators ranging from 2850 to 2650 cm^{-1}. A hydrogen-bonded O−D

DOI: 10.1021/acs.jpclett.7b00273
J. Phys. Chem. Lett. 2017, 8, 1272−1277

stretching mode is only observed for n = 4, leading to band D (2352 cm^{-1}), which extends from 2550 down to 2200 cm^{-1}. Band D appears very broad, typical of a hydrogen-bonded oscillator.[33]

To determine the (global) minimum-energy structures of the clusters we performed DFT calculations. Global optimization with a genetic algorithm[34] was followed by local refinement with the B3LYP functional[35] and a TZVPP basis set.[36] The resulting structures are shown in the right part of Figure 1. The $Al_3O_4^+$ ion (Figure 2) has C_{3v} symmetry and consists of a triply

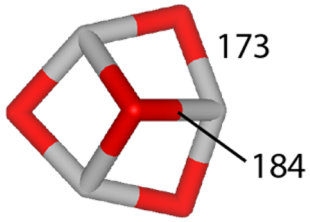

Figure 2. Minimum-energy (B3LYP/TZVPP) structure of $Al_3O_4^+$ with distances in pm.

coordinated O atom (μ_3-O) capping a six-membered (−Al−O−)$_3$ ring.[18] This structural motif is also found for n = 3, whereas for n = 1 and 2 the structures are planar.

For all systems the reaction with D_2O,

$$[Al_3O_4]^+ + nD_2O \rightarrow [Al_3O_4(D_2O)_n]^+$$

is highly exothermic and exclusively involves dissociative D_2O adsorption. In absolute terms, the adsorption energy per D_2O molecule, $\Delta E/n$, decreases from 437 to 275 kJ/mol with increasing n. Additional local minimum structures are shown in Figures S4−S9 of the Supporting Information. The lowest energy structure containing at least one molecularly adsorbed D_2O molecule for n = 1, 2, 3, and 4 lies 199, 69, 139, and 12 kJ/mol, respectively, above the global minimum-energy structure.

The simulated IR spectra for the lowest energy isomers are shown in the lower panels of each system in Figure 1. The B3LYP/TZVPP wavenumbers and intensities are convoluted with a Gaussian line-shape function (fwhm: 10 cm^{-1}) to account for the spectral width of the laser radiation as well as rotational broadening. The O−D wavenumbers are scaled by the factor 0.9732, which has been derived as

$$^1/_2(\nu_s + \nu_{as})/^1/_2(\omega_s + \omega_{as})$$

from the observed fundamentals ν of D_2O[29] and the calculated harmonic wavenumbers ω. For the smaller systems (n < 2) the messenger species used in the experiment has a significant effect on the IR spectrum and therefore the calculated spectrum of the complex containing the messenger species is shown (see SI for a comparison of all simulated IR spectra). The computed spectra are in very good agreement with the experimental ones over both spectral regions probed, which confirms that the global minimum-energy structures have been found. The remaining discrepancies are mainly attributed to less efficient photodissociation at lower photon energies, which lie close to or even below the dissociation limit of the ion-messenger tag complex (e.g., band K in the n = 1 spectrum).

Dissociative adsorption of the first D_2O molecule leads to the planar bicyclic structure with two terminal OD groups bound to individual Al atoms (see Figure 1). Their vibrations are weakly coupled into a symmetric (calc. 2797 cm^{-1}) and an antisymmetric (calc. 2798 cm^{-1}) combination, and are assigned to the intense band A at 2806 cm^{-1}. The small peak labeled † in Figure 1 corresponds to excitation of the perturbed D−D stretching mode of the D_2 tag. This mode is IR-forbidden in a free D_2 molecule (2994 cm^{-1}),[34] but obtains IR-intensity and is substantially red-shifted (152 cm^{-1}) due to the polarization interaction with the ion. Peaks G to I are assigned to Al_2−(μ_2-O) stretching modes. The highest energy bands E and F arise from the symmetric and antisymmetric stretches involving the two Al−OD moieties. An in-plane mode of Al_3−(μ_3-O) coupled with the Al−O−D bending modes is predicted at lower energies (515 cm^{-1}) and attributed to peak K at 539 cm^{-1}.

Dissociative adsorption of the second D_2O molecule leads to a planar six-membered ring structure with three terminal OD groups, each bound to one of the three Al atoms, and one bridging Al_2−(μ_2-OD) group (see Figure 1). The terminal O−D modes calculated at 2801, 2793, and 2791 cm^{-1} contribute to a single band (A), which is 6 cm^{-1} red-shifted with respect to the corresponding band for n = 1. The bridging μ_2-O−D mode is about 140 cm^{-1} shifted to lower wavenumbers (2659 cm^{-1}) and assigned to band B (2651 cm^{-1}). The two IR-active modes highest in energy in the fingerprint region (calc. 1109 and 1079 cm^{-1}) are all Al_2−(μ_2-O) stretching modes and assigned to bands E (1104 cm^{-1}) and F (1077 cm^{-1}). Band G (981 cm^{-1}) most likely arises from the Al−OD stretch modes. The in-plane bend of the bridging Al_2−(μ_2-OD) is calculated at 826 cm^{-1} (δ^D) and assigned to band H (819 cm^{-1}), while bands I (694 cm^{-1}) and J (625 cm^{-1}) are assigned to Al_2−(μ_2-O) stretches (calc. 689 cm^{-1}, 620 cm^{-1}). Ring deformation modes δ (Al_2−(μ_2-OD) out-of-plane motions) are predicted below 500 cm^{-1}.

The lowest energy structure found for n = 3 (C_3) is similar to the C_{3v} structure of n = 0, but contains only 4-fold coordinated Al-atoms, due to the presence of three terminal hydroxyl groups. The remaining three D atoms form three bridging (μ_2-OD) moieties. This high symmetry is reflected in the predicted IR spectrum, which contains only five IR-active bands. These are assigned, from high to low energy, to the terminal O−D stretches (A), bridging μ_2-O−D stretches (B), Al−OD stretches (E), in-plane bends involving predominantly the bridging Al_2−(μ_2-OD) groups (F) and the Al_3−(μ_3-O) stretches (G).

The n = 4 structure is the first that contains an intramolecular hydrogen bond which leads to additional features in the O−D stretching region. Bands C (2750 cm^{-1}, calc. 2759 cm^{-1}) and D (2352 cm^{-1}, calc. 2359 cm^{-1}) in the experimental spectrum are assigned to the terminal and bridging (μ_2) OD groups, which act as hydrogen-bond acceptor and donor, respectively. Bands A and B are attributed to stretches of terminal and bridging μ_2-OD groups, respectively, analogous to the IR spectra of the smaller clusters. The many bands in the fingerprint region reflect the heterogeneity of the n = 4 structure. The Al_2−(μ_2-O) stretching modes (calc. 965, 942, 929, and 739 cm^{-1}) are assigned to bands E (942 cm^{-1}) and G (743 cm^{-1}). Bands F (790 cm^{-1}), H (698 cm^{-1}) and partially G (743 cm^{-1}) stem from the in-plane bending modes of the bridging (μ_2-OD) groups (calc. 794, 768, and 702 cm^{-1}). A shoulder at band F might result from the hydrogen bonded Al_2−(μ_2-OD) bending mode (calc. 852 cm^{-1}). Additional Al_2−(μ_2-O) modes are predicted at lower energies (≤650 cm^{-1}) and attributed to the remaining bands I−L.

The assignment of the reported vibrational spectra allows identifying characteristic IR absorption regions for different

DOI: 10.1021/acs.jpclett.7b00273
J. Phys. Chem. Lett. 2017, 8, 1272−1277

modes (see Figure S10 of the Supporting Information). The O−D stretching region extends roughly from 2810 cm^{-1} down to 2650 cm^{-1} and can be grouped into two nonoverlapping regions. The terminal O−D stretches are found in the narrow region between 2810 and 2790 cm^{-1}. The bridging μ_2-O−D stretches lie well separated between 2750 and 2650 cm^{-1}. A hydrogen-bonded O−D stretch is observed further to red, below 2550 cm^{-1}.

Figure 3 shows the wavenumbers of the OD group as a function of the formal oxygen charge, and compares the present

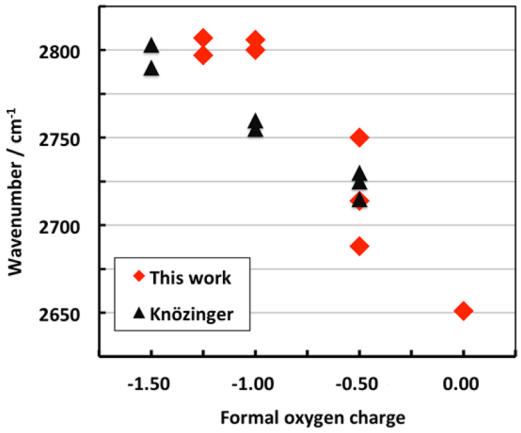

Figure 3. Observed wavenumbers for O−D stretching vibrations of $[Al_3O_4(D_2O)_n]^+$ gas-phase clusters and different solid aluminas[10,30] as a function of the formal oxygen charge.

results with the data collected by Knözinger[10,30] for different alumina surfaces. The formal oxygen charge is obtained from the charge of fully reduced oxygen atoms (−2) and the sum of the electrostatic bond strengths of the adjacent aluminum atoms/ions. The latter is defined as the cation charge divided by its coordination number. For a terminal hydroxyl group on a hexa-coordinated Al^{3+} ion the formal oxygen charge is $-2 + {}^3/_6 = -1.5$, whereas on a tetra- and tricoordinated Al^{3+} ion, as in the clusters with $n = 3$ and $n = 1$, respectively, it is $-2 + {}^3/_4 = -1.25$ and $-2 + {}^3/_3 = -1.0$. For the bridging Al_2-(μ_2-OD) group in $n = 2$ it is $-2 + 2\ (+{}^3/_3) = 0$. Figure 3 shows that the O−D stretching wavenumbers reported for different alumina phases,[30] 2803−2715 cm^{-1}, are within the same range as our results for the gas phase $[Al_3O_4(D_2O)_{1-4}]^+$ clusters. Moreover, our results for the gas phase model systems support the assignment based on the trend with the formal oxygen charge.

The unambiguous assigment reached for the model systems provides guidance for understanding O−D stretching vibrations in more complex alumina systems. For example, only three of the five O−D vibrations observed by VSF spectroscopy on an α-Al_2O_3 (0001) surface,[6] at 2790 ± 3, 2764 ± 5, and 2729 ± 5 cm^{-1} fall into the range of terminal and bridging O−D groups, respectively, established by our experiments on gas phase model systems and previous experiments for alumina surfaces. The two additional bands, observed by VSF[6] spectroscopy at 2910 and 2900 cm^{-1}, are 100 cm^{-1} outside the range of O−D wavenumbers established here for surface O−D groups on alumina, which calls for additional work on this problem.

The results of the present study can also be used to assist the assignment of O−H stretching modes of different aluminum oxide/water systems. We make use of the empirical wavenumber-scaling factor 1.36 determined for all-H and all-D isotopologues of the protonated water pentamer, which is close to that obtained for isolated O−H versus O−D oscillators (1.37).[31] This yields estimated spectral windows for (free) terminal and bridging O−H stretching modes of 3820−3800 and 3740−3600 cm^{-1}, respectively. The OH data between 3800 and 3700 cm^{-1} collected by Knözinger and Ratnasamy[10] for different alumina phases fall into this region. The IR peaks at 3742 and 3704 cm^{-1} reported[9] for α-Al_2O_3 as well as the broad peak at 3730−3720 cm^{-1} in the high resolution electron energy loss spectra (HREELS) of the Al_2O_3 (0001) surface[37] indeed correspond to bridging hydroxyl groups.

In conclusion, the unambiguous assignment for gas phase model systems of O−D (O−H) stretching wavenumbers to terminal (μ_1) and bridging (μ_2) hydroxyl groups in aluminum oxide/water systems sheds new light on controversial assignments for solid Al_2O_3 phases. Moreover, the good agreement between experimental and calculated O−D wavenumbers lends credit to DFT calculations also for more complex systems.

EXPERIMENTAL METHODS

IRPD experiments are conducted on an ion trap tandem mass spectrometer described elsewhere.[38,39] Aluminum-oxide cation/water complexes are formed in a dual gas-channel laser-vaporization source (see Figure S1 of the Supporting Information).[40] The beam of ions passes a 4 mm diameter skimmer, is then collimated in a buffer-gas-filled radio frequency (RF) decapole ion-guide, and ions of interest are selected according to their mass/charge ratio using a quadrupole mass-filter. The mass-selected beam is focused into a cryogenically cooled RF ring electrode ion-trap. The trap is continuously filled with 1% D_2 in He buffer gas at a trap temperature of 13−15 K, which allows for the accumulation and thermalization of the trapped ions. Inside the ion trap, ions undergo three-body collisions with the buffer gas, which promote the formation of weakly bound ion−D_2 complexes.[41] After 199 ms all ions are extracted from the ion trap and focused in the center of the extraction region of a time-of-flight (TOF) mass spectrometer, where they are irradiated by an intense and wavelength-tunable IR laser pulse. When resonant with a vibrational transition, the parent ions can absorb one (or more) photon(s), leading to loss of one or more messenger molecules via intramolecular vibrational predissociation. For the larger water complexes ($n > 2$) ion-messenger complex formation is not efficient and the vibrational spectra are measured via infrared multiple photon photodissociation (IRMPD). In this case, multiple dissociation channels are observed with D_2O loss being the most efficient at low energy fluence followed by the loss of multiple D_2O molecules (see Figures S2 and S3 of the Supporting Information).

The IR free electron laser FHI FEL[42] is used as a light source for the wavelength from 3.3 to 5 μm (IRMPD) and from 8.3 to 23 μm with a bandwidth between 0.3 and 0.6% root-mean-square of the central wavelength. Laser light for IRPD experiments in the O−D stretch region, from 3.3 to 4 μm, is produced by an OPO/OPA laser system (Laser Vision) pumped by a seeded Nd:YAG laser (Continuum, Powerlite DLS-8000).[43] IR spectra are recorded by averaging over 60 TOF mass spectra per wavelength step. The intensities are normalized to the total number of parent (I_P) and fragment (I_F) ions, to account for fluctuations in the total ion signal. The photodissociation cross sections σ_{IRPD} and σ_{IRMPD} are obtained as described elsewehere.[44]

DOI: 10.1021/acs.jpclett.7b00273
J. Phys. Chem. Lett. 2017, 8, 1272−1277

COMPUTATIONAL METHODS

Low energy isomers of $Al_3O_4^+ (H_2O)_n$ (n = 0−4) are generated using a genetic algorithm (GA) and employing the BP86 functional[45,46] together with a split valence polarized basis set SVP (Al: 4s3p1d, O: 3s2p1d).[36] For each composition 2000 isomers are generated. The ten most stable structures each are then reoptimized with the B3LYP functional[35] and a triple-ζ plus polarization (TZVPP) basis set (Al: 5s5p3d1f, O: 5s3p2d1f), named "def2" in the Turbomole library.[36] There were no significant changes of structures or relative energies on reoptimization.

As a genetic algorithm the hybrid approach of the dodo program[34,47] is employed. DFT calculations are performed with the TURBOMOLE 7.1 programs[48,49] assuming always a closed shell electronic structure. IR spectra are computed within the double harmonic approximation as implemented in TURBOMOLE. Frequencies above 2000 cm^{-1} were scaled with the factor 0.9732 to account for anharmonic effects and systematic errors of the harmonic force constants.

ASSOCIATED CONTENT

Supporting Information

The Supporting Information is available free of charge on the ACS Publications website at DOI: 10.1021/acs.jpclett.7b00273.

Additional experimental details, experimental spectra compared to computed spectra for different isomers, tables of experimental and calculated vibrational wave numbers, characteristic IR absorption regions, total energies, and Cartesian atomic coordinates of global energy minimum structures (PDF)

AUTHOR INFORMATION

Corresponding Authors

*E-mail: knut.asmis@uni-leipzig.de.
*E-mail: js@chemie.hu-berlin.de.

ORCID

Wieland Schöllkopf: 0000-0003-0564-203X
Knut R. Asmis: 0000-0001-6297-5856
Joachim Sauer: 0000-0001-6798-6212

Notes

The authors declare no competing financial interest.

ACKNOWLEDGMENTS

This work has been supported by the German Research Foundation (DFG) within CRC 1109 "Metal Oxide−Water Interfaces". Xiaowei Song thanks the Alexander-von-Humboldt Foundation for a postdoctoral research fellowship.

REFERENCES

(1) Trueba, M.; Trasatti, S. P. γ-Alumina as a support for catalysts: A review of fundamental aspects. *Eur. J. Inorg. Chem.* **2005**, *2005*, 3393−3403.

(2) Franks, G. V.; Gan, Y. Charging behavior at the alumina−water interface and implications for ceramic processing. *J. Am. Ceram. Soc.* **2007**, *90*, 3373−3388.

(3) Álvarez, J.; Serrano, C.; Hill, D.; Martínez-Pastor, J. Real-time polarimetric optical sensor using macroporous alumina membranes. *Opt. Lett.* **2013**, *38*, 1058−1060.

(4) Brown, G. E. How Minerals React with Water. *Science* **2001**, *294*, 67−69.

(5) Lemire, C.; Meyer, R.; Henrich, V. E.; Shaikhutdinov, S.; Freund, H. J. The surface structure of Fe_3O_4(1 1 1) films as studied by CO adsorption. *Surf. Sci.* **2004**, *572*, 103−114.

(6) Kirsch, H.; Wirth, J.; Tong, Y. J.; Wolf, M.; Saalfrank, P.; Campen, R. K. Experimental characterization of unimolecular water dissociative adsorption on alpha-alumina. *J. Phys. Chem. C* **2014**, *118*, 13623−13630.

(7) Tong, Y.; Wirth, J.; Kirsch, H.; Wolf, M.; Saalfrank, P.; Campen, R. K. Optically probing Al—O and O—H vibrations to characterize water adsorption and surface reconstruction on α-alumina: An experimental and theoretical study. *J. Chem. Phys.* **2015**, *142*, 054704.

(8) Wirth, J.; Kirsch, H.; Wlosczyk, S.; Tong, Y. J.; Saalfrank, P.; Campen, R. K. Characterization of water dissociation on a-Al_2O_3(1-(1)over-bar02): theory and experiment. *Phys. Chem. Chem. Phys.* **2016**, *18*, 14822−14832.

(9) Morterra, C.; Magnacca, G. A case study: surface chemistry and surface structure of catalytic aluminas, as studied by vibrational spectroscopy of adsorbed species. *Catal. Today* **1996**, *27*, 497−532.

(10) Knözinger, H.; Ratnasamy, P. Catalytic aluminas - Surface models and characterization of surface sites. *Catal. Rev.: Sci. Eng.* **1978**, *17*, 31−70.

(11) Digne, M.; Sautet, P.; Raybaud, P.; Euzen, P.; Toulhoat, H. Use of DFT to achieve a rational understanding of acid−basic properties of γ-alumina surfaces. *J. Catal.* **2004**, *226*, 54−68.

(12) Sauer, J.; Freund, H.-J. Models in catalysis. *Catal. Lett.* **2015**, *145*, 109−125.

(13) Asmis, K. R.; Sauer, J. Mass-selective vibrational spectroscopy of vanadium oxide cluster ions. *Mass Spectrom. Rev.* **2007**, *26*, 542−562.

(14) Song, X.; Fagiani, M. R.; Gewinner, S.; Schöllkopf, W.; Asmis, K. R.; Bischoff, F. A.; Berger, F.; Sauer, J. Gas phase structures and charge localization in small aluminum oxide anions: Infrared photodissociation spectroscopy and electronic structure calculations. *J. Chem. Phys.* **2016**, *144*, 244305.

(15) Song, X.; Fagiani, M. R.; Gewinner, S.; Schöllkopf, W.; Asmis, K. R.; Bischoff, F. A.; Berger, F.; Sauer, J. Gas phase vibrational spectroscopy of $(Al_2O_3)_{1-6}AlO_2^-$. *ChemPhysChem* **2017**, DOI: 10.1002/cphc.201700089.

(16) Mascaritolo, K. J.; Gardner, A. M.; Heaven, M. C. Autodetachment spectroscopy of the aluminum oxide anion dipole bound state. *J. Chem. Phys.* **2015**, *143*, 114311.

(17) Sierka, M.; Döbler, J.; Sauer, J.; Zhai, H.-J.; Wang, L.-S. The $[(Al_2O_3)_2]^-$ anion cluster: electron localization−delocalization isomerism. *ChemPhysChem* **2009**, *10*, 2410−2413.

(18) Santambrogio, G.; Janssens, E.; Li, S.; Siebert, T.; Meijer, G.; Asmis, K. R.; Döbler, J.; Sierka, M.; Sauer, J. Identification of Conical Structures in Small Aluminum Oxide Clusters: Infrared Spectroscopy of $(Al_2O_3)_{1-4}(AlO)^+$. *J. Am. Chem. Soc.* **2008**, *130*, 15143−9.

(19) Stößer, G.; Schnöckel, H. The molecules AlO_2, $Al(O_2)_2$, and $Al(O_2)_3$: experimental and quantum-chemical investigations on the oxidation of aluminum atoms. *Angew. Chem., Int. Ed.* **2005**, *44*, 4261−4264.

(20) Akin, F. A.; Jarrold, C. C. Addition of water and methanol to $Al_3O_3^-$ studied by mass spectrometry and anion photoelectron spectroscopy. *J. Chem. Phys.* **2003**, *118*, 5841−5851.

(21) Akin, F. A.; Jarrold, C. C. Reactivity of $Al_3O_3^-$ cluster toward H_2O studied by density functional theory. *J. Chem. Phys.* **2004**, *120*, 8698−8706.

(22) Das, U.; Raghavachari, K.; Jarrold, C. C. Addition of water to $Al_5O_4^-$ determined by anion photoelectron spectroscopy and quantum chemical calculations. *J. Chem. Phys.* **2005**, *122*, 014313.

(23) Das, U.; Raghavachari, K. Interaction of water, methanol, and ammonia with $Al_xO_y^-$: A comparative theoretical study of $Al_5O_4^-$ versus $Al_3O_3^-$. *J. Chem. Phys.* **2007**, *127*, 154310.

(24) Tenorio, F. J.; Murray, I.; Martínez, A.; Klabunde, K. J.; Ortiz, J. V. Products of the addition of water molecules to $Al_3O_3^-$ clusters: Structure, bonding, and electron binding energies in $Al_3O_4H_2^-$,$Al_3O_5H_4^-$,$Al_3O_4H_2$, and $Al_3O_5H_4$. *J. Chem. Phys.* **2004**, *120*, 7955−7962.

DOI: 10.1021/acs.jpclett.7b00273
J. Phys. Chem. Lett. 2017, 8, 1272−1277

(25) Guevara-García, A.; Martínez, A.; Ortiz, J. V. Addition of water, methanol, and ammonia to $Al_3O_3^-$ clusters: Reaction products, transition states, and electron detachment energies. *J. Chem. Phys.* **2005**, *122*, 214309.
(26) Guevara-García, A.; Martínez, A.; Ortiz, J. V. Sequential addition of H_2O, CH_3OH, and NH_3 to $Al_3O_3^-$: A theoretical study. *J. Chem. Phys.* **2007**, *126*, 024309.
(27) Wang, Z. C.; Weiske, T.; Kretschmer, R.; Schlangen, M.; Kaupp, M.; Schwarz, H. Structure of the Oxygen-Rich Cluster Cation $Al_2O_7^+$ and its Reactivity toward Methane and Water. *J. Am. Chem. Soc.* **2011**, *133*, 16930−16937.
(28) Johnson, J. R. T.; Panas, I. Water adsorption and hydrolysis on molecular Al oxides and hydroxides-solvation versus cluster formation. *Phys. Chem. Chem. Phys.* **2001**, *3*, 5482−5488.
(29) Tennyson, J.; Bernath, P. F.; Brown, L. R.; Campargue, A.; Császár, A. G.; Daumont, L.; Gamache, R. R.; Hodges, J. T.; Naumenko, O. V.; Polyansky, O. L.; et al. IUPAC critical evaluation of the rotational-vibrational spectra of water vapor. Part IV. Energy levels and transition wavenumbers for $D_2{}^{16}O$, $D_2{}^{17}O$, and $D_2{}^{18}O$. *J. Quant. Spectrosc. Radiat. Transfer* **2014**, *142*, 93−108.
(30) Knözinger, H. Hydrogen bonds in systems of adsorbed molecules. In *Hydrogen Bond*, Schuster, P.; Zundel, G.; Sandorfy, C., Eds.; North Holland: Amsterdam, 1976; Vol. *III*, p 1263.
(31) Fagiani, M. R.; Knorke, H.; Esser, T. K.; Heine, N.; Wolke, C. T.; Gewinner, S.; Schöllkopf, W.; Gaigeot, M.-P.; Spezia, R.; Johnson, M. A.; et al. Gas phase vibrational spectroscopy of the protonated water pentamer: the role of isomers and nuclear quantum effects. *Phys. Chem. Chem. Phys.* **2016**, *18*, 26743−26754.
(32) Douberly, G. E.; Walters, R. S.; Cui, J.; Jordan, K. D.; Duncan, M. A. Infrared Spectroscopy of Small Protonated Water Clusters, $H^+(H_2O)_n$ (n = 2−5): Isomers, Argon Tagging, and Deuteration. *J. Phys. Chem. A* **2010**, *114*, 4570−4579.
(33) Wolke, C. T.; DeBlase, A. F.; Leavitt, C. M.; McCoy, A. B.; Johnson, M. A. Diffuse Vibrational Signature of a Single Proton Embedded in the Oxalate Scaffold, $HO_2CCO_2^-$. *J. Phys. Chem. A* **2015**, *119*, 13018−13024.
(34) Sierka, M.; Döbler, J.; Sauer, J.; Santambrogio, G.; Brummer, M.; Wöste, L.; Janssens, E.; Meijer, G.; Asmis, K. R. Unexpected structures of aluminum oxide clusters in the gas phase. *Angew. Chem., Int. Ed.* **2007**, *46*, 3372−5.
(35) Becke, A. D. Density-functional thermochemistry. III. The role of exact exchange. *J. Chem. Phys.* **1993**, *98*, 5648.
(36) Weigend, F.; Ahlrichs, R. Balanced basis sets of split valence, triple zeta valence and quadruple zeta valence quality for H to Rn: Design and assessment of accuracy. *Phys. Chem. Chem. Phys.* **2005**, *7*, 3297−305.
(37) Coustet, V.; Jupille, J. High-resolution electron-energy-loss spectroscopy of isolated hydroxyl groups on α-Al2O3(0001). *Surf. Sci.* **1994**, *307−309*, 1161−1165.
(38) Goebbert, D. J.; Meijer, G.; Asmis, K. R. 10K ring electrode trap - Tandem mass spectrometer for infrared spectroscopy of mass selected ions. *AIP Conf. Proc.* **2008**, *1104*, 22−29.
(39) Goebbert, D. J.; Garand, E.; Wende, T.; Bergmann, R.; Meijer, G.; Asmis, K. R.; Neumark, D. M. Infrared spectroscopy of the microhydrated nitrate Ions $NO_3^-(H_2O)_{1-6}$. *J. Phys. Chem. A* **2009**, *113*, 7584−7592.
(40) Wende, T. *Gas Phase Infrared Photodissociation Spectroscopy of Mass-Selected Ionic Clusters: Metal Oxides and Microhydrated Anions*; Freie Universität: Berlin, 2012.
(41) Brümmer, M.; Kaposta, C.; Santambrogio, G.; Asmis, K. R. Formation and photodepletion of cluster ion-messenger atom complexes in a cold ion trap: Infrared spectroscopy of VO^+, VO_2^+, and VO_3^+. *J. Chem. Phys.* **2003**, *119*, 12700−12703.
(42) Schöllkopf, W.; Gewinner, S.; Junkes, H.; Paarmann, A.; von Helden, G.; Bluem, H.; Todd, A. M. M. The new IR and THz FEL facility at the Fritz Haber Institute in Berlin. *Proc. SPIE* **2015**, *9512*, 95121L.
(43) Bosenberg, W. R.; Guyer, D. R. Broadly tunable, single-frequency optical parametric frequency conversion system. *J. Opt. Soc. Am. B* **1993**, *10*, 1716−22.
(44) Heine, N.; Asmis, K. R. Cryogenic ion trap vibrational spectroscopy of hydrogen-bonded clusters relevant to atmospheric chemistry. *Int. Rev. Phys. Chem.* **2015**, *34*, 1−34. Corrigendum: 2016, *35*, 507.
(45) Becke, A. D. Density-functional exchange-energy approximation with correct asymptotic behavior. *Phys. Rev. A: At., Mol., Opt. Phys.* **1988**, *38*, 3098−3100.
(46) Perdew, J. P. Erratum: Density-functional approximation for the correlation energy of the inhomogeneous electron gas. *Phys. Rev. B: Condens. Matter Mater. Phys.* **1986**, *34*, 7406−7406.
(47) Sierka, M. Synergy between theory and experiment in structure resolution of low-dimensional oxides. *Prog. Surf. Sci.* **2010**, *85*, 398−434.
(48) TURBOMOLE V7.1 2016, a development of University of Karlsruhe and Forschungszentrum Karlsruhe GmbH available from http://www.turbomole.com..
(49) Ahlrichs, R.; Bär, M.; Häser, M.; Horn, H.; Kölmel, C. Electronic structure calculations on workstation computers: The program system Turbomole. *Chem. Phys. Lett.* **1989**, *162*, 165−169.

DOI: 10.1021/acs.jpclett.7b00273
J. Phys. Chem. Lett. 2017, 8, 1272−1277